Cell Tissue Res (2002) 308:193–203
DOI 10.1007/s00441-002-0542-y

REGULAR ARTICLE

Dora E. Vega-Salas · Manuel Fernandez III
Keyvan Nouri

Characterization and changes of a chromosomal-scaffolding protein in human epithelia

Received: 16 July 2001 / Accepted: 8 February 2002 / Published online: 12 April 2002

Abstract Chromosomal-scaffolding proteins exert DNA structural functions during mitosis, and gene regulatory functions such as RNA splicing/polymerization and DNA replication in interphase, allowing the progression of the cell cycle. Recently, it has been reported that topoisomerases play a key role in DNA repair, suggesting an additional regulatory mechanism of the chromosome structure on DNA metabolism and cell cycle checkpoints. Despite the progress made toward the understanding of the genome organization and expression, few changes have been reported in the chromosome scaffold of malignant cells associated with the cancer phenotype. In a previous work, we reported LFM-1 protein (Licensing Factor Model-1) as a chromosomal-scaffold component transiently associated with mitotic chromosomes in MDCK (Madin Darby canine kidney) epithelial cells (Vega-Salas and Salas 1996). In this work, we explore LFM-1 expression in human epithelia with contrasting tumorigenicity during the progression of the cell cycle. Although cell metabolic labeling shows synthesis of a common 87-kDa LFM-1 precursor during G_2-phase in both non-tumorigenic and cancer cells, surprisingly, the post-translational LFM-1 chromosome-bound polypeptide displays a different apparent molecular weight and binding to chromosomes in the cancer phenotype. The finding of a highly phosphorylated LFM-1 60-kDa form with abnormal binding to chromosomes in human carcinoma cells suggests a structural/regulatory role(s) of the chromosome-scaffold/matrix in DNA metabolism in cancer-related events of cell proliferation.

Keywords Chromosomal-scaffold · Cancer · Epithelia · Cell cycle · Proliferation · Human

D.E. Vega-Salas (✉) · M. Fernandez III
Department of Cell Biology and Anatomy,
1600 NW 10th Ave. (R-124), University of Miami,
School of Medicine, PO Box 016960, Miami, FL 33101, USA
e-mail: dsalas@med.miami.edu
Tel.: +1-305-2436947, Fax: +1-305-5457166

K. Nouri
Department of Dermatology, University of Miami,
School of Medicine, Miami, FL 33101, USA

Introduction

Chromosomal matrix or scaffold (Berezney and Coffey 1974; Paulson and Laemmli 1977; Earnshaw et al. 1985; Gasser et al. 1986) is the chromosome protein web that fastens to matrix/scaffold highly conserved repetitive DNA sequences named matrix regions (MARs) and scaffold regions (SARs) (Gasser et al. 1989; Von Kries et al. 1991; Saitoh et al. 1995; Wei et al. 1998), and organizes the higher-order chromatin loops. It has been reported that this network is involved in the control of DNA functions such as chromosomal condensation, chromatid segregation (Mirkovich et al. 1984; Uemura et al. 1987; Wright and Shatten 1990; Saitoh et al. 1995; Subramanian et al. 1998), and chromatin transcription and methylation (Hirano and Mitchison 1991; Stein et al. 1996). Also, a regulatory role in DNA replication has been proposed, and it is reported that the specific binding of MAR/SAR proteins to DNA affects the nearby gene expression (Dijkwel et al. 1986; Gasser et al. 1989; Wright and Shatten 1990; Zlatanova and van Holde 1992; Hamlin 1992; Pernov et al. 1998).

Cancer cells differ from the normal parental tissues in the fast, deregulated cell cycle progression. They seem to be partially or totally independent from extracellular signals (Durkin and Whitfield 1984; Guadagno and Assoian 1991; Takeichi 1993) and from intracellular regulatory cascades of phosphorylations (Kirchner 1992; Prevostel et al. 1998), events that would control molecular changes and subcellular distribution of nuclear and cytoplasmic proteins involved in cell proliferation (Nasmyth et al. 1991; Getzember and Coffey 1991; Hatakeyama and Weinberg 1995; Getzember et al. 1996; de Belle et al. 1998; Saville and Watson 1998). Over the last few years, mutated hyperphosphorylated nuclear-matrix proteins have been proposed to play a role in neoplastic processes (Kanuja et al. 1993; Keesee et al. 1994; Yang et al. 1997; Zeng et al. 1997). However, although a correlation with cancer phenotype exists, no conclusive evidence has confirmed their oncogenic function.

In a previous paper, we identified a protein bound to mitotic chromosomes in non-tumorigenic canine kidney cells. We named it LFM-1 (Licensing Factor Model-1) by its resemblance to MCM2–7 proteins, a group of molecules with DNA replication licensing activity. We described a LFM-1 58-kDa polypeptide associated with the chromosomal and nuclear fractions in mitosis and G_1-phase of cell cycle, and also reported its resistance to extraction procedures (3', 5'-diiodosalicylic acid and high ionic strength), a biochemical operational definition for scaffolding/matrix components. In addition, we described the peripheral and axial distribution of the 58-kDa LFM-1 polypeptide on chromatids and the nuclear localization in G_1 nuclei by standard epifluorescence and confocal microscopy. Although analysis of interphase cells revealed the 58-kDa LFM-1-kDa polypeptide included in G_1 nuclei, and a 87-kDa cytoplasmic polypeptide in G_2-phase cells (Vega-Salas and Salas 1996), no relationship among these bands was studied. As a preliminary set of data for this study, the chromosomal-scaffolding features were explored and confirmed in human epithelial cells. In the present work, we analyze the synthesis, post-translational processing and subcellular localization of LFM-1 chromosomal-scaffold component in human epithelia with contrasting tumorigenicity. Our results support a group of nuclear proteins with transient cellular translocations during the post-translational processing, strong chromosome binding (Gasser et al. 1986; Hennesy et al. 1990) and structural/regulatory functions on DNA metabolism (Hernandez-Verdun and Gautier 1994) during cell proliferation events (Stillman et al. 1988; Dohrman et al. 1992; Blow 1993; Coverley et al. 1993; Brazas and Stillman 1993; Madine et al. 1995). In addition, our findings show an LFM-1 variant with abnormal mass and binding to chromosomes in the cancer phenotype, but, most importantly, they suggest that the reported structural and functional changes in chromosomal-scaffold components may be involved in deregulated cell-cycle events of cancer proliferation.

Materials and methods

Cell culture and synchrony

Human breast MCF-10A non-tumorigenic epithelial cells (ATCC CRL) (Soule et al. 1990) were grown in D-MEM/F-12, 10% (v/v) horse serum (Gibco, Grand Island, NY), 100 ng/ml cholera toxin, 5 ng/ml epidermal growth factor, and 20 µg/ml hydrocortisone (Gibco, BRL, Gaithersburg, MD). Human breast MCF-7 carcinoma cells (Soule et al. 1973) were kindly provided by I. Luthy (IBYME, Conicet). In both cases, the culture media were supplemented with 1 mM non-essential amino acids, 1 mM sodium pyruvate, 10 µg/ml insulin (Gibco), 100 IU penicillin, and 100 µg/ml streptomycin (Sigma Chemical Co., St. Louis, MO) and kept in 95% air-5% CO_2, 37°C, in DMEM/F-12, 10% (v/v) fetal bovine serum (Gibco). The cultures were harvested weekly by dissociation in 0.25% trypsin/2 mM ethylenediaminetetraacetic acid (EDTA). The cells were plated at subconfluency ($2–6\times10^4$ cells/cm^2) and kept under standard culture conditions 24 h before the experiments.

The span of the cell-cycle phases for each cell line was determined in preliminary experiments by flow cytometry of synchronized cultures. Cells in G_1-phase were obtained by incubation in starvation media (DMEM no-isoleucine, 10% dialyzed horse or fetal calf serum, and 2 mM L-glutamine) for ~36–48 h. Cultures in S-phase were achieved by cell-cycle arrest in G_1/S-phase with 2.5 mM hydroxyurea/aphidicolin as described by Nishimoto et al. (1981) and release in normal media. Alternatively, we used 400 µM mimosine in DMEM complete media supplemented with 10% heat inactivated serum for ~12 h (Dijkwel et al. 1991) to obtain cells in S-phase. To synchronize cells in G_2-phase, the cultures were first arrested in G_1/S and then released from treatment for different times as per the span of cell-cycle phases determined for each cell line. Thus, MCF-10A were released for 3 h (S) and 8 h (G_2); or for 2 h (S) and 5 h (G_2) in the case of MCF-7 cells. Synchronization in metaphase was achieved by incubation with 0.06 µg/ml nocodazole (Sigma) for ~17–24 h (Vega-Salas and Salas 1996). Before synchronization experiments, MCF10A and MCF-7 (~4×10^4 cells/cm^2) were grown on either glass coverslips or plastic roller bottles for 24 or 72 h. To improve the sample homogeneity of collected mitotic cells due to the different attachment of each cell line by nocodazol treatment, we included an additional procedural step of vigorous shake-off of MCF-10A cells, and gentle collection of mitotic MCF-7 cells before the experiments. The success of cell synchrony was determined by a fluorescence-activated cell sorter (FACS) as described below, and by a number of mitotic images observed under the microscope.

FACS analysis

MCF-10A and MCF-7 cells were synchronized as described above, treated with RNase A, stained with propidium iodide, and sorted using a Beckton-Dickinson Facster Plus cell cytometer. To estimate the success of the synchronization, the cellular DNA content was quantified in parallel samples by flow cytometry. The efficiency of synchronization of MCF-10A cells was: G_1-phase, 84–87%; S/G_2-phase, 77–82%; mitosis, 72–76%. MCF-7 cells showed: 68–73% (G_1-phase); 61–65% (S/G_2-phases), and 65–69% (M-phase). The average of cell synchrony during a complete cell cycle was 72–87% and 61–73% for each phenotype, respectively.

Metabolic labeling

Subconfluent cells were synchronized in different phases of the cell cycle as described previously (Vega-Salas and Salas 1996). Pulse-chase metabolic labeling was performed with ~1.5 mCi [^{35}S]methionine-[^{35}S]cysteine/ml for ~30 min at 37°C, 95% air, 5% CO_2 on a rocker, after rinsing in DMEM methionine/cysteine free media for 15 min at the start of each cell-cycle phase. Two samples were taken per phase, and immunoprecipitated using LFM-1 MAb and normal mouse IgGs (negative control), electrophoresed in 10% sodium dodecyl sulfate polyacrylamide gel electrophoresis (SDS-PAGE), dried for ~3 h at 68°C, and exposed for ~17 h (PhosphorImager, Molecular Dynamics, Sunnyvale, CA).

Additional time-course experiments were performed by incubation of synchronized cultures in G_2-phase with ~3.5 mCi [^{35}S]methionine-[^{35}S]cysteine/ml for ~2 h. Two points were then taken per cell-cycle phase, immunoprecipitated with LFM-1 MAb, and processed as described above.

Hybridoma production

LFM-1 hybridoma was prepared as described previously (Vega-Salas and Salas 1996) by fusion of BALB-c mice splenocytes and NS-1 myeloma cells. Briefly, the cell pellets – mostly nuclear – from MDCK (Madin Darby canine kidney) homogenates were fixed in 3% formaldehyde (from paraformaldehyde, PFA) for 30 min at room temperature. They were then washed twice in Hank's saline buffer solution, and injected intraperitoneally in mice. The screenings were performed by solid-phase radioimmunoassay on monolayers and immunofluorescence on M-phase synchronized cell populations. The reactive immunoglobulins were typed as IgG_1.

Cell fractionation: nuclear, chromosomal and cytoplasmic fractions

Nuclear and cytoplasmic fractions were obtained from non-synchronized and synchronized cells from both cell lines as described previously (Mirkovich et al. 1984; Vega-Salas and Salas 1996).The metaphase chromosome fraction was purified from nocodazole-treated cultures (Gasser and Laemmli 1987). Briefly, subconfluent cultures were then grown in 75-cm^2 plastic flasks (1.3×10^7 cells) or 850-cm^2 roller bottles ($1.5–2\times10^8$ cells). Before the experiments, the cells were rinsed twice and scraped in ice-cold phosphate saline buffer supplemented with an antiprotease inhibitor cocktail [1 mM phenylmethylsulfonyl fluoride (PMSF), 2 µg/ml aprotinin, 10 µg E-64, and 1 µM pepstatin] (Calbiochem, La Jolla, CA), centrifuged and resuspended twice in isolation buffer (3.75 mM TRIS-HCl, 0.5 mM spermine, 0.125 mM spermidine, 20 mM KCl, 1% (v/v) thiodiglycol, and 0.5 mM EDTA/KOH, 0.2 mM PMSF, 5 µg/ml aprotinin, pH 7.4) (Gasser and Laemmli 1987; Vega-Salas and Salas 1996) and isolation buffer supplemented with 0.1% digitonin at 4°C for 3 min (by 15 s alternated sonication). The nuclei were finally pelleted at 1,100 *g* for 15 min. The resulting supernatants were ultracentrifuged (Beckman L8–70 M) at 100,000 *g* at 4°C for 1 h, yielding a cytoplasmic (membrane) pellet. Finally, both (nuclear and cytoplasmic) pellets were resuspended in SDS sample buffer, 0.1% β-mercaptoethanol, heated at 95°C for 3 min, and analyzed by SDS electrophoresis in 8–10% polyacrylamide gels as described previously (Vega-Salas and Salas 1996).

To purify mitotic chromosomes and prophase nuclei, we synchronized cultures in M-phase, harvested them by vigorous shake-off, centrifuged at 200 *g* for 10 min, and washed twice in solution I: hypotonic buffer (7.5 mM TRIS Cl, 40 mM KCl, 1 mM EDTA/KOH, 0.1 mM spermine, 0.5 mM spermidine, pH 7.4), 1% (v/v) thiodiglycol, and antiprotease inhibitor cocktail (mentioned above) containing 5 µg/ml aprotinin. The cells were then centrifuged at 800 *g* for 5 min, resuspended in ice-cold solution II ×2 hypotonic buffer [1% (v/v) thiodiglycol, 5 µg/ml aprotinin, 1 mM PMSF, 0.1% digitonin], disrupted with ten strokes of a Dounce homogenizer and let stand on ice for 10 min. The homogenates were placed over a 5–70% glycerol gradient in solution III, 1:2 hypotonic buffer in 2d H_2O (1% thiodiglycol, 0.1% digitonin, antiprotease cocktail), and centrifuged in a swing-out rotor for 5 min at 200 *g*, followed by 15 min at 700 *g*. The chromosomes recovered in the lower part of the gradient, were centrifuged again into 5 ml cushion of 70% glycerol at 3,500 *g* for 15 min and stored in this cushion at –20°C before immunofluorescence or PAGE processing. In both cases, the fractions were monitored by phase microscopy and immunoblot using polyvalent antibodies against tubulin and cytokeratins for control of cytoplasmic contamination. No further purification procedures were required even in the case of MCF-10A cells, which showed a higher resistance to fractionation than MCF-7 cells.

Indirect immunofluorescence

The standard method for immunofluorescence labeling of whole tissue culture cells has been described previously (Vega-Salas et al. 1987; Vega-Salas and Salas 1996). Synchronized cells as described above were fixed, permeabilized in 0.2% Triton X-100/0.15% saponin or 70/30% methanol/acetone at –20°C, and processed with LFM-1 MAb supernatant (1:3 in PBS) and 20 µg/ml affinity purified goat anti-mouse IgGs coupled to fluorescein (with minimal cross-reactivity to human proteins, Jackson Labs., West Grove, PA). Negative controls were incubated with 10 µg/ml mouse preimmune IgGs. Isolated nuclei or chromosomes were processed by standard immunofluorescence procedures but after incubations the samples were washed by ~3 min spinning/resuspension cycles. During the procedures, nuclei were kept in PBS supplemented with 1 mM $MgCl_2$ and 0.1 mM $CaCl_2$ while chromosomes were maintained in hypotonic buffer (15 mM TRIS-HCl, 80 mM KCl, 2 mM EDTA/KOH, 0.2 mM spermine, 0.1 mM spermidine, pH 7.4, 1% thiodiglycol, 5 µg/ml aprotinin, and 1 mM PMSF) (Gasser and Laemmli 1987) to avoid aggregation. When colocalization with chromatin was aimed at, the samples were pretreated with 1 mg/ml RNase-A (Sigma) for 15 min at room temperature immediately after the second antibody and prior to the incubation with 1 mg/ml propidium iodide. Finally, cells, nuclei or isolated chromosomes were thoroughly washed before mounting in a mix of 1:1 polyvinyl alcohol (20% polyvinyl alcohol, 15% glycerol, 1% *n*-propyl gallate in PBS) and Slowfade (Molecular Probes, Eugene, OR) as described previously (Vega-Salas and Salas 1996). The images were visualized under a Leitz DM RB epifluorescence microscope (Leica, Wetzar, Germany) using T-Max 400 ASA or Ektachrome 160T film (Kodak). To control cytoskeletal contaminations, we incubated the cells with rabbit polyvalent antibodies against tubulin, actin and cytokeratins, and affinity purified goat against rabbit IgGs, fluorescein isothiocyanate (FITC) or peroxidase-labeled second antibodies.

Confocal microscopy

Isolated nuclei from MCF-10A and MCF-7 cells were processed by immunofluorescence as described above, and analyzed by laser confocal microscopy (Molecular Dynamics, Sunnyvale, CA). Usually, 40–62 confocal sections were taken (0.1 µm thick) throughout two detection channels and three-dimensionally reconstructed using image analysis software (Molecular Dynamics).

SDS-PAGE and immunoblot

Human biopsies from normal tissues and carcinomas were obtained from the Tissue Procurement facility of the Sylvester Comprehensive Cancer Center, University of Miami. The samples ranging 130 to 250 mg were kept in liquid nitrogen until homogenization in 150–300 µl ×4 sample buffer, 6 M urea for 4–6 min on ice. Normalization of protein content was done by the Bradford test prior to plating the gels. Aliquots of homogenates of human biopsies or fractions of tissue culture cells (20–120 µl/lane) were electrophoresed by standard 8–10% SDS PAGE (Laemmli 1970), electroblotted onto nitrocellulose (Towbin et al. 1979), and developed by a peroxidase-detection chemiluminescence system (ECL, Amersham, Bucks, UK). The immunoreagents were LFM-1 MAb (1:3 in PBS), affinity purified goat anti-mouse IgGs-biotin conjugated (1:2000, Sigma), and Extravidin-peroxidase (1:2500, Sigma) in 0.1% Tween-20/PBS, 1 mM $MgCl_2$, 0.1 mM $CaCl_2$. The tissue biopsies reported in this paper were as follows (Fig. 4, from left to right): normal breast and ductal breast carcinoma (same patient); breast adenocarcinoma, normal colon; colon adenocarcinoma; normal breast; poorly differentiated breast adenocarcinoma; normal skin; skin melanoma; normal kidney; kidney cell carcinoma; and kidney Wilms' carcinoma.

To determine the phosphoepitopes in LFM-1 polypeptides, MCF-10A and MCF-7 cells were grown at subconfluency for ~24 h, harvested on ice-cold PBS supplemented with protease inhibitors, immunoprecipitated using LFM-1 MAb, and processed by SDS-PAGE and Western blot. The nitrocellulose sheets were developed by standard chemiluminescence procedures using anti-serine, threonine, and tyrosine MAbs (Sigma, cat. 3430, 3555 and 3300) and goat anti-mouse, peroxidase-labeled IgGs.

Alkaline phosphatase

Confluent non-synchronized $1.5–2\times10^7$ MCF-10A and MCF-7 cells were harvested by scraping in the presence of antiprotease inhibitor cocktail, homogenized and fractionated in nuclear and cytoplasmic pellets as described above. Each fraction was resuspended in 100 µl final volume (200 mM CO_3Na_2/CO_3HNa buffer, pH 9.8), supplemented with 0.5 mM $MgCl_2$, and separated into two aliquots. One of these samples was incubated with 80 DEA units of type VII-NL bovine alkaline phosphatase (orthophosphoric-monoester phosphohydrolase) from intestine mucosa (Sigma, cat. no. 3131) in 50 mM TRIS HCl, 1 mM $MgCl_2$, 0.1 mM $ZnCl_2$, 1 mM spermidine, pH 8.9, for 40 min at 37°C. The reaction was

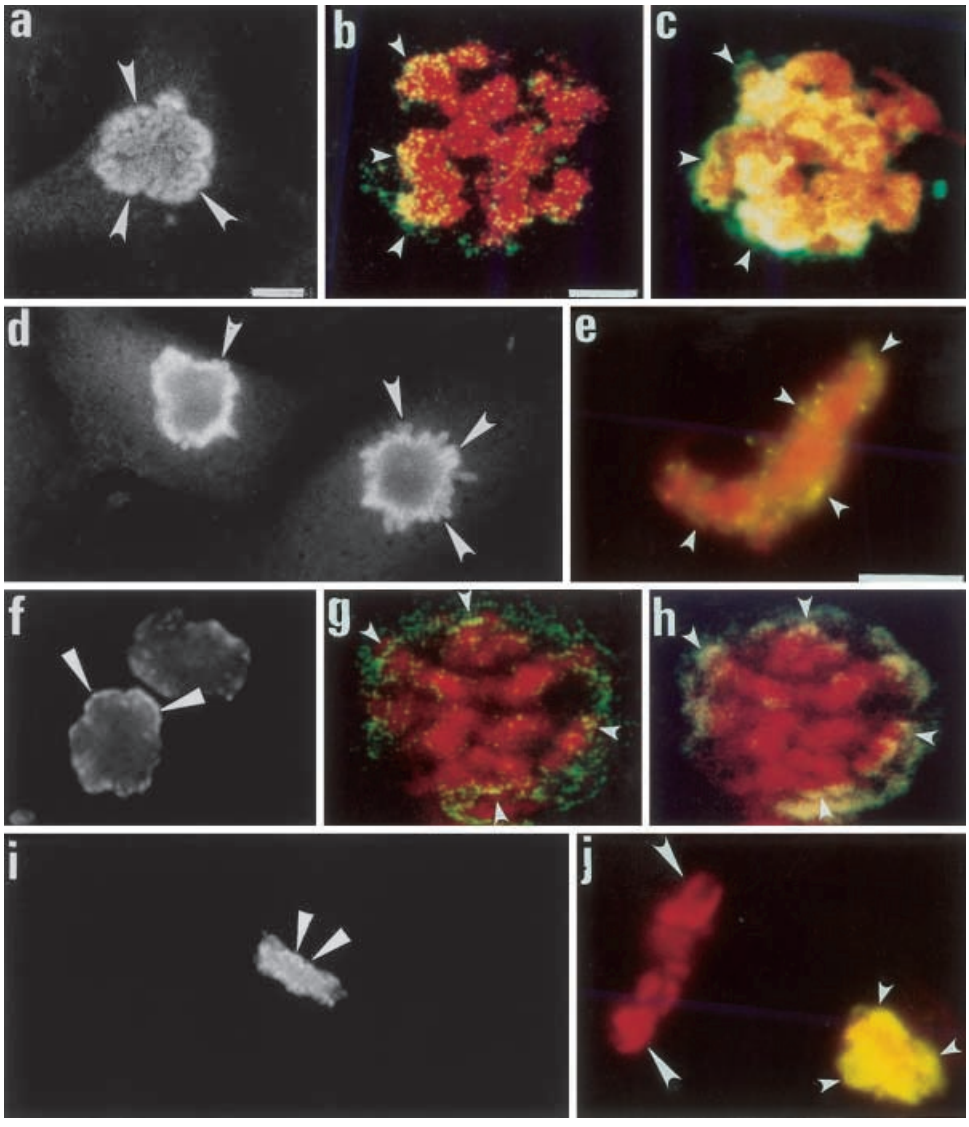

then stopped in 6 mM TRIS, 0.8 mM EDTA, 150 mM NaCl, pH 7.5, the enzyme was removed by two cycles of centrifugation/resuspension, and the final pellets were processed by PAGE and immunoblot.

Results

LFM-1 protein abnormally binds to mitotic chromosomes in tumor cells

LFM-1 subcellular distribution and association with chromosomes in human epithelia were analyzed in human subconfluent MCF-10A and MCF-7 cells during the cell cycle by standard epifluorescence and confocal microscopy. The brightest LFM-1 signal was observed on mitotic chromosomes (Fig. 1a, d and f, i). A continuous intense LFM-1 mark was observed in the periphery of condensing chromosomes in prophase nuclei (Fig. 1a, white arrowheads) and surrounding metaphase plaques (Fig. 1d, white arrowheads) in MCF-10A non-tumorigenic cells consistent with our previous observations in canine

Fig. 1a–j Subcellular nuclear and chromosomal distribution of LFM-l signal during mitosis in human MCF-10A non-tumorigenic and MCF-7 carcinoma cells. Subconfluent cultures were synchronized in M-phase, fixed, permeabilized, and processed by immunofluorescence. **a–e** MCF-10A non-tumorigenic cells; **f–j** MCF-7 carcinoma cells. **a–c, f–h** Nucleus in prophase; **d, i** chromosome metaphase plates; **e, j** isolated mitotic chromosomes. **b, g** Confocal nuclear sections; **c, h** and tridimensional reconstitution images. Prophase nuclei from actively growing MCF-10A and MCF-7 cells were isolated, processed by immunofluorescence (LFM-1 protein, fluorescein, green channel) and propidium iodide (DNA, red channel), and analyzed by epifluorescence **(a, f)** or confocal laser microscopy **(b, c, g, h)**. **b, g** Single medial confocal optical sections (0.1 µm thick) and **c, h** the corresponding 3D reconstitution (by look-through projections) of the stack of sections. Note a brighter LFM-1 signal decorating condensing MCF-10A **(a–c)** but not MCF-7 **(f–h)** chromosomes on both epifluorescence **(a, f)** and confocal images (**b, c** and **g, h**) (*arrowheads*). However, although nuclear envelope/chromosome contact areas were positive in both cell phenotypes, a decreased LFM-1 signal was observed in carcinoma cells. Isolated metaphase chromosomes from non-tumorigenic cells **(e)** displayed uniform LFM-1/fluorescein signal (*green*) surrounding the chromatids (*red*) while chromosomes from MCF-7 cells **(j)** displayed a heterogeneous fluorescence pattern often with no LFM-1 labeling (**j**, *big white arrowheads*). *Scale bars* 5 µm **(a, d, f, i)**, 2.5 µm **(e–j)**, 3 µm **(b, c, g, h)**

kidney non-tumorigenic cells (Vega-Salas and Salas 1996). However, in contrast, a decreased labeling of LFM-1 was suspected in nuclei of MCF-7 carcinoma cells (Fig. 1f, i).

To further investigate the extent of LFM-1 association with chromosomes in the cancer phenotype, purified chromosome fractions of MCF-10A and MCF-7 cultures in M-phase were comparatively analyzed by immunofluorescence and confocal microscopy. These preparations contained some prophase nuclei that were included in this study (Fig. 1b, c, g, h). Approximately 90 prophase nuclei per cell line were examined colocalizing DNA (propidium iodide after RNase treatment, red channel) and LFM-1 epitopes (fluorescein, green channel). Consistent with the images from unfractionated cultures (Fig. 1a, f), confocal tridimensional images displayed LFM-1 epitopes overlapping the condensing chromosomes in localized nuclear peripheral areas in MCF-10A cells. Despite a grossly conserved nuclear fluorescence pattern of LFM-1 in both cell lines, a faint signal in MCF-7 tumor cells was observed (Fig. 1c, h, arrows), which was further confirmed by the analysis of the confocal sections (Fig. 1b, g). Since images in b and g are 0.1-µm confocal sections, the general reduction of LFM-1 epitopes was evident in both the periphery and axis of the chromatids in cancer cells (Fig. 1b). Consistent with these findings, isolated mitotic chromosomes from MCF-7 carcinoma cells showed a heterogeneous LFM-1 labeling. The fluorescence ranged from bright/undetectable signal (Fig. 1j, big white arrowheads), including a less common configuration of patchy positive areas clearly contrasting with the homogeneous subcellular distribution observed in non-tumorigenic cells (Fig. 1i). As a conclusion of these studies, LFM-1 protein displays a notorious heterogeneous and decreased chromosome binding to chromosomes in cancer cells (Fig. 1c, h, yellow signal, white arrowheads).

Carcinoma cells display a molecular LFM-1 variant associated with mitotic chromosomes

To identify the LFM-1 molecular species bound to mitotic chromosomes, unsynchronized cultures from both cell lines were fractionated in nuclear and cytoplasmic pellets as described previously (Vega-Salas and Salas 1996). The nuclei – referred to hereafter as nuclear fraction – and the postnuclear supernatant (membrane pellet) (Mirkovich et al. 1984; Gasser and Laemmli 1987) were processed by SDS-PAGE (Fig. 2A). The purified nuclear fraction of MCF-10A cells showed a major 58-kDa and secondary 65- and 87-kDa LFM-1 bands (Fig. 2N, asterisk). In contrast, the equivalent Western blot of MCF-7 nuclei displayed a 60-kDa polypeptide (arrowhead) and similar 65- and 87-kDa minor bands. Because LFM-1 signal detected in the nuclear fraction comprised all LFM-1 polypeptides associated with nuclei and chromosomes during a complete cell cycle, we decided to further discriminate the specific LFM-1 polypeptide(s)

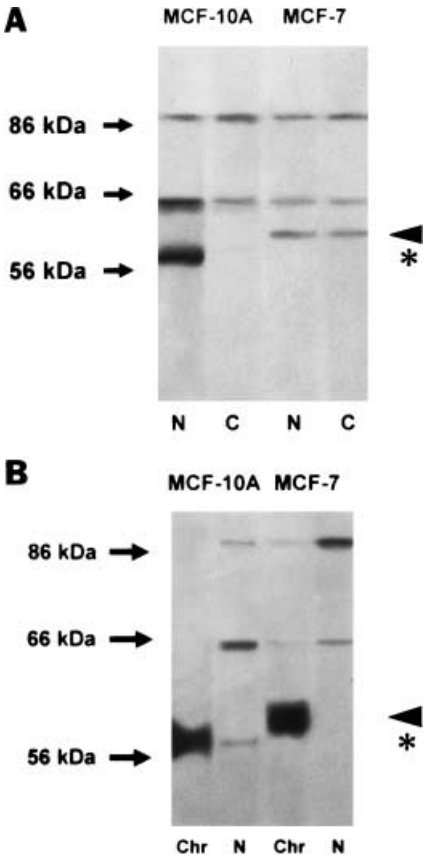

Fig. 2A, B LFM-1 molecular species associated with the nuclear (*N*) and cytoplasmic (*C*) fractions **(A)** and chromosome fraction (**B**, *Chr*) in human non-tumorigenic (*MCF-10A*) and tumorigenic (*MCF-7*) cells. Unsynchronized cultures **(A)** were harvested, fractionated, and the nuclear and cytoplasmic pellet processed by SDS-PAGE and immunoblot. A 58-kDa LFM-1 band is identified in the nuclear fraction of MCF-10A non-tumorigenic cells (*). MCF-7 carcinoma cells instead display a 60-kDa LFM-1 polypeptide (*arrowhead*). Cells synchronized in M-phase by nocodazol treatment were homogenized and the chromosomes isolated (*Chr*). The remaining attached cells to the substrate (in interphase) were then scraped and fractionated to obtain the nuclear pellet (*N*). A major 58-kDa band is the major LFM-1 polypeptide identified in the chromosome (*Chr*) fraction of MCF-10A non-tumorigenic cells (*), while a 60-kDa band was detected in mitotic chromosomes of MCF-7 carcinoma cells (*arrowhead*) (*arrows* 86, 66, and 56 kDa: molecular weight markers)

bound to chromosomes during M-phase. Accordingly, the pattern of bands from the purified chromosome fraction in M-phase was compared with the one in unsynchronized cultures (Fig. 2A, N, B, Chr). As a result, mitotic chromosomes of MCF-10A non-tumorigenic cells displayed a defined unique 58-kDa LFM-1 major band (Fig. 2Chr, asterisk). In contrast, MCF-7 carcinoma cells showed a major 60-kDa LFM-1 polypeptide (Fig. 2Chr, arrowhead) and modest minor 65- and 87-kDa polypeptides. These observations were extended and confirmed in normal and cancer biopsies from human breast, colon, skin and kidney epithelia. A correlated 58-kDa LFM-1 electrophoretic band was obtained from biopsies of normal epithelia in contrast

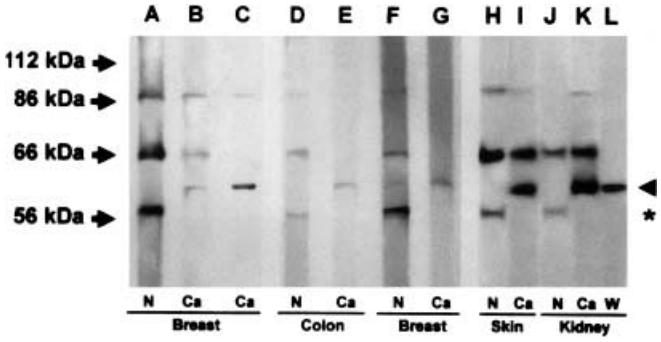

Fig. 3 LFM-1 polypeptides from whole extracts of human biopsies processed by SDS-PAGE. Tissue samples were electrophoresed, blotted and incubated with LFM-1 MAb and processed by chemiluminescence (*asterisk* 58-kDa LFM-1 band, *arrowhead* 60-kDa LFM-1 variant in carcinoma cells, *N* normal, *Ca* carcinoma, *W* Wilms' tumor). Each lane corresponds to a single biopsy. Note the relationship between the 58-kDa LFM-1 polypeptide and normal phenotype, and the 60-kDa band in cancer biopsies (*arrows* standard molecular weight markers)

with a 60-kDa polypeptide in carcinomas from several organs. Figure 3 shows the correlation between both LFM-1 forms in tissues and tumor biopsies.

The consistent findings in human tissues point to the 58-kDa band as the major LFM-1 polypeptide in normal epithelia, and the 60-kDa band as its correlated chromosome polypeptide in cancer cells, and also suggest an involvement of the chromosome scaffold/matrix in the cancer phenotype.

A common LFM-1 precursor is synthesized in G_2 in both non-tumorigenic and cancer cells

The identification of a 58-kDa LFM-1 chromosome band in non-tumorigenic cells and a 60-kDa variant in cancer cells compelled us to discriminate between unrelated molecules with similar LFM-1 antibody recognition and differential post-translational processing of a common LFM-1 precursor (phenotype-dependent feature). As a first approach, MCF-10A and MCF-7 cells were synchronized in G_1-, S-, and G_2-phases of the cell cycle, metabolically labeled with [^{35}S]methionine/cysteine, immunoprecipitated with LFM-1 MAb and analyzed by autoradiogram. A unique 87-kDa LFM-1 polypeptide was detected in both cell lines in G_2-phase (Fig. 4A, B, asterisks), which correlated with the highest molecular band detected in cell homogenates of unsynchronized cultures (Figs. 2, 3). No additional bands were detected even with longer pulse labeling, and/or film exposure through a complete cell cycle, supporting the idea that the 87-kDa polypeptide is the unique LFM-1 precursor. In addition, quantification of the [^{35}S]-labeling of LFM-1 87-kDa bands was performed in both phenotypes using Image-Quant software. The immunoprecipitation controls

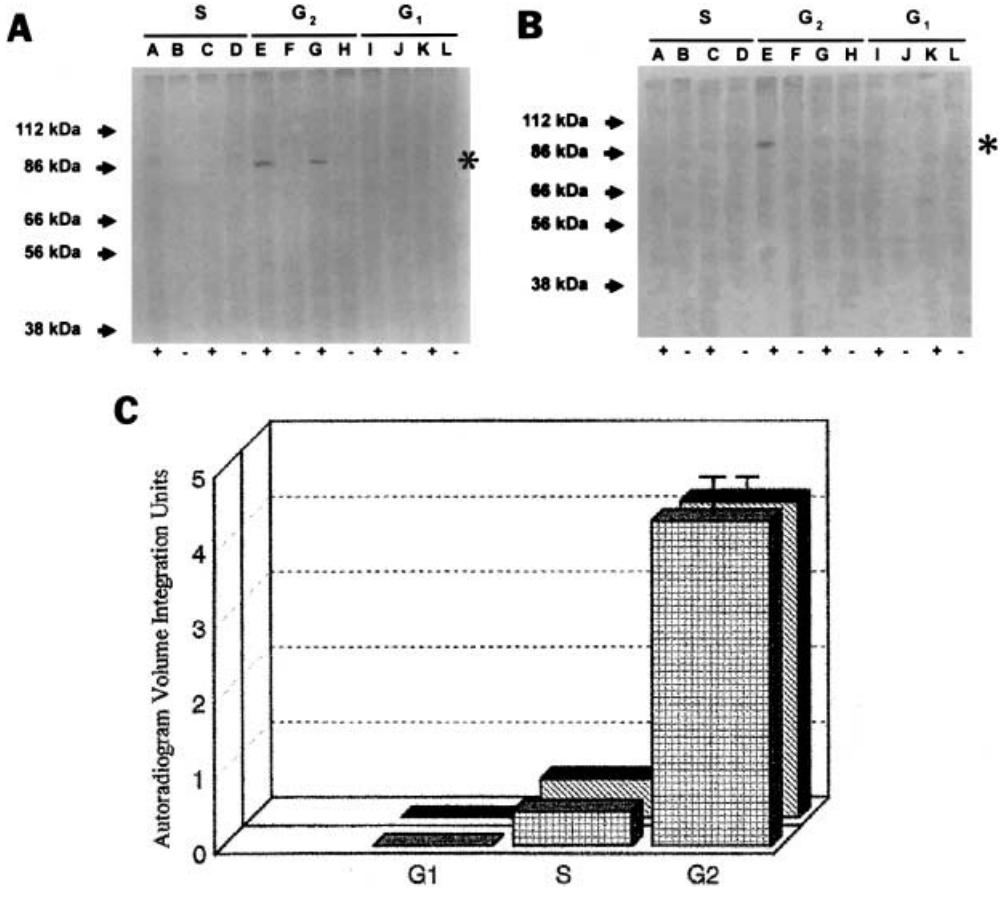

Fig. 4 Identification of a single LFM-1 precursor in MCF-10A **(A)** and MCF-7 **(B)** cells by [^{35}S]methionine/cysteine labeling and immunoprecipitation with LFM-1 MAb during the cell cycle **(A, B)**. **C** Quantification of [^{35}S]methionine/cysteine labeling of the 87-kDa bands in **A** and **B**. Synchronized cells were labeled and analyzed in G_2-, G_1- and S-phases of cell cycle. The synthesis of an 87-kDa LFM-1 precursor was detected in G_2-phase in both cell lines (*asterisks*). Immunoprecipitation of LFM-1 with LFM-1 MAb (+) is in *lanes A, C, E, G, I, and K*. Negative controls (–) are in *B, D, F, H, J, and L lanes*. Note that no bands are detected in the remaining phases of cell cycle. **C** An 87-kDa signal was measured using Image Quant software. The background from the corresponding negative control was subtracted. Note the synthesis of a common LFM-1 precursor in both cell lines during the G_2-phase of the cell cycle

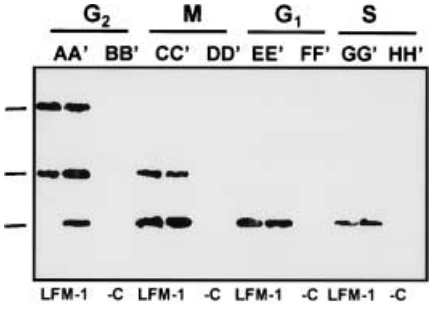

Fig. 5 Time course metabolic labeling of the 87-kDa LFM-1 precursor during a complete cell cycle in MCF-10A. Cells synchronized in G_2-phase were [^{35}S]methionine/cysteine labeled and released for various times. Two points were taken per cell-cycle phase. The samples were immunoprecipitated, electrophoresed, and developed in a PhosphorImager as described above. Samples in *A,A', C,C', E,E'* and *G,G'* were immunoprecipitated with LFM-1 MAb. Negative controls for immunoprecipitation (*-C*, normal mouse IgGs) are in lanes *B,B', D,D', F,F'* and *H,H'*. *Bars* point to standard molecular weights of 86, 66 and 56 kDa. The autoradiogram in MCF-7 cells displayed an equivalent pattern of bands, but a 60-kDa polypeptide was observed instead of the 58-kDa band (not shown)

were subtracted as background from each line in the autoradiogram (Fig. 4C). Although the efficiency of cell synchronization was higher for MCF-10A cells, the corrected values (integration unit per synchronized cell) showed higher synthesis of LFM-1 precursor in carcinoma cells (see "Efficiency of cell synchronization" in "Materials and methods").

LFM-1 polypeptides are post-translational products of the 87-kDa precursor

To study the relationship among LFM-1 polypeptides, synchronized cultures in G_2 were pulse-labeled with [^{35}S]methionine/cysteine for ~2 h and released for different times based on the previously determined cell cycle span of each cell line. Two samples were taken per cell cycle phase, immunoprecipitated with LFM-1 MAb, and processed by SDS-PAGE and autoradiogram (Fig. 5). We found a rapid post-translational modification of the 87-kDa- to 65-kDa and 58-kDa LFM-1 polypeptides during G_2-phase. Consequently, the 58-kDa band was the major band detected in mitosis and afterwards in G_1- and S-phases (Fig. 5A', C, C', E, E', G). MCF-7 carcinoma cells instead displayed a 60-kDa polypeptide from the onset of M-phase until S-phase, and a similar equivalent general pattern of LFM-1 bands consistently reported in previous experiments (Fig. 2A, B, arrowheads).

Altogether, these results show the appearance of a 60-kDa LFM-1 post-translational variant in cancer cells despite the synthesis of a common 87-kDa precursor in G_2-phase and a similar cell-cycle profile of post-translational processing in both cell phenotypes.

LFM-1 polypeptides are differentially phosphorylated. Those mostly containing Tyr and Thr are sensitive to dephosphorylation.

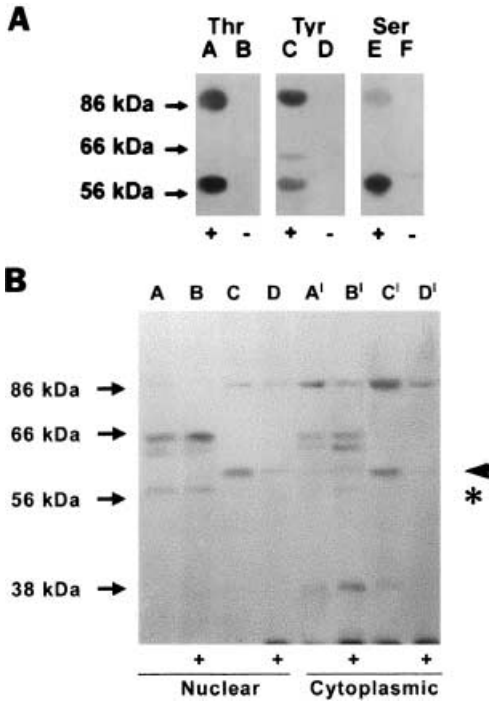

Fig. 6 Determination of tyrosine, threonine, and serine phosphoepitopes in LFM-1 polypeptides **(A)**, and changes in mass of LFM-1 polypeptides by alkaline phosphatase treatment **(B)**. **A** LFM-1 polypeptides were immunoprecipitated from whole cell extracts of unsynchronized cultures. Negative controls were carried out with normal mouse IgGs. The elutes were electrophoresed and processed by immunoblot using monoclonal antibodies against phosphothreonine, phosphotyrosine and phosphoserine. *A, C, E* Immunoprecipitation with LFM-1 MAb. *B, D, F* Immunoprecipitation control. Tyrosine phosphorylation is mostly detected in 87-kDa LFM-1 precursor, while phosphorylation in threonine is present in the 87-kDa LFM-1 precursor and the 58-kDa chromosome-associated band as well. However, serine phosphorylation is mainly observed in the 58-kDa LFM-1 chromosome/nuclear polypeptide. **B** Confluent unsynchronized MCF-10A (*A, B, A', B'*) and MCF-7 (*C, D, C', D'*) cells were harvested, homogenized and fractionated in nuclear and cytoplasmic pellets. One of each sample was incubated with alkaline phosphatase (+), and the final pellets were processed by PAGE and immunoblot. Note the degradation of LFM-1 87- and 65-kDa cytoplasmic polypeptides in both cell phenotypes with a shift in the mass of only the 60-kDa LFM-1 chromosome form in the nuclear fraction. *Arrowhead* points to 60-kDa band; *asterisk* indicates 58-kDa LFM-1 polypeptide

To explore the relationship among LFM-1 bands and correlate it with the subcellular localization, we first determined the amino acid phosphoepitopes in LFM-1 polypeptides (Fig. 6A). Parallel to changes in the apparent molecular weight of LFM-1 polypeptides, variations in its amino-acid phosphorylation were detected in unsynchronized MCF-10A cells by immunoprecipitation and electrophoresis/Western blotting. LFM-1 phosphoepitopes were assayed, reacting the nitrocellulose membranes with antiphosphoserine, phosphothreonine, and phosphotyrosine MAbs, and chemiluminescence. The analysis of epitope phosphorylation of LFM-1 polypeptides did not reveal any ostensible difference in equivalent LFM-1 bands in both cell lines. While the 87-kDa band was phosphorylated in tyrosine, threonine and serine, the

minor intermediate 65-kDa LFM-1 polypeptide displayed phosphorylation in tyrosine and threonine, and the major 58/60-kDa chromosomal forms showed mostly marked serine phosphoepitopes (Fig. 6A).

To further determine the extent of involvement of dephosphorylation processes in the post-translational modifications of LFM-1 polypeptides, we explored the sensitivity of LFM-1 polypeptides to alkaline phosphatase treatment. Accordingly, MCF-10A and MCF-7 cells were homogenized and separated into nuclear and cytoplasmic fractions as described in "Materials and methods." One aliquot of each sample was treated with alkaline phosphatase (Fig. 6B, +) and a parallel one kept as control (Fig. 6B, –). It is important to mention that the common treatment of all samples with a common batch of alkaline phosphatase provided an internal reliable control for the purity of the enzyme potentially contaminated with antiproteases. No major changes in mass of LFM-1 nuclear bands were detected in either cell line by alkaline phosphatase treatment (Fig. 6B, A, B, C, D) despite an increased degradation of the 60-kDa polypeptide in the nuclear fraction of MCF-7 cells, resulting in small polypeptides in front of the gel (Fig. 6B, D). The treatment of the cytoplasmic pellets by alkaline phosphatase, however, dramatically changed the regular pattern of LFM-1 bands in both cells. The 87-kDa LFM-1 precursor was significantly degraded by the enzymatic treatment to an evident intermediate 65-kDa LFM-1 band in MCF-10A cells (Fig. 6B, A', B'). However, although a dephosphorylation process was evident in the cytoplasmic fraction of MCF-7 carcinoma cells, the 87-kDa LFM-1 precursor significantly degraded mostly to unspecific polypeptides in the front of the gel, with no intermediate products (Fig. 6C', D').

These results show parallel changes in the common post-translational phosphorylation processing of the 87-kDa LFM-1 precursor in both cell phenotypes. However, they suggest a dissimilar sensitivity of the 87-kDa precursor and intermediate products to dephosphorylation in both cell phenotypes.

Discussion

LFM-1 in human tissues

In this work, we identify and study LFM-1 protein in human cell lines and tissues, analyze its synthesis and post-translational processing, and report on differences in the post-translational chromosome form in cancer cells. Despite lineage and species differences, LFM-1 apparent molecular weight and subcellular distribution in human normal epithelia (breast, kidney, colon, and skin) correlate with that previously reported in MDCK non-tumorigenic dog kidney epithelium (Vega-Salas and Salas 1996), supporting the idea that LFM-1 is a well conserved protein. Most importantly, this study reports a 60-kDa LFM-1 form which displays consistent changes in its relative molecular mass and binding to chromosomes in a variety of human cancer cells. Altogether, these results and the transient LFM-1 binding to chromosomes during progression of the cell cycle suggest that the 60-kDa LFM-1 variant may be related to the cancer phenotype and play a role in malignant cell proliferation.

Relationship between LFM-1 bands: synthesis and post-translational processing; shift in the mass of the LFM-1 chromosome form in cancer cells

The first hypothesis one can postulate to explain the multiband pattern of LFM-1 polypeptides is the monoclonal recognition of a common epitope in unrelated polypeptides. However, our results strongly suggest it is unlikely. Cell metabolic labeling showed only one LFM-1 precursor during the entire cell-cycle. If other unspecific polypeptides had been recognized by the LFM-1 antibody, it should have resulted in the appearance of additional bands, which was not the case. In addition, experiments of time-course cell labeling displayed an LFM-1 pattern of bands correlating with the one reported in unsynchronized cultures. These results suggest that the 60- and 58-kDa LFM-1 chromosome polypeptides originate from a common 87-kDa LFM-1 precursor by means of cytoplasmic post-translational phosphorylation processing. Most importantly, they show molecular and functional changes in the 60-kDa post-translational polypeptide in cancer cells. In this regard, a correlation has been reported between modest changes in the molecular weight of proteins and their DNA binding ability after post-translational modifications (Luscher and Eisenman 1992). Often these modifications involve phosphorylation processes that regulate complementary proteolytic cleavages of the polypeptide chain (Reddy et al. 1991). Currently, we cannot rule out a change in the primary structure of LFM-1 precursor, nor in the post-translational machinery of cancer cells for the abnormal mass and binding to chromosomes in the cancer phenotype.

It has been reported that dephosphorylation processing in tyrosine and threonine epitopes with parallel serine phosphorylation exert regulatory key functions on subcellular distribution, mass, and functions of a number of cytoplasmic proteins (Reddy et al. 1991; Tyers et al. 1992; Ng et al. 1992; Swarup and Radha 1992; Johnson and Foley 1993; Elvira et al. 1993). The simultaneous molecular and functional changes on LFM-1 polypeptides with parallel cell-cycle-dependent cellular translocations during post-translational phosphorylation processing support these data.

Similarities of LFM-1 with known proteins; potential functions

Interestingly, the results in this paper partially resemble a few proteins in the literature which are cell proliferation related. One of them, SWI5, shows a comparable cell-cycle temporal translocation: it enters into the nucleus in

M-phase (the mitosis in yeast is closed), binds to chromosomes in anaphase, remains nuclear during G_1-phase (exerting regulatory functions at the onset of start) and is degraded afterwards (Blow 1993; Coverley et al. 1993). SATB1 (specific A-T binding) is a recently reported nuclear-matrix protein (Dickinson et al. 1992; Yanagisawa et al. 1996; de Belle et al. 1998). Despite some common features with LFM-1 such as binding to MAR/SAR areas of DNA, and a similar apparent molecular weight, there is no significant sequence homology between these proteins.

As a chromosomal-scaffold component, LFM-1 protein may have a function in the higher order chromatin folding, and also a role in gene expression. To date, our findings suggest that LFM-1 might exert function(s) on DNA metabolism during progression of the cell cycle somewhat comparable to MCM2–7 DNA replication licensing factors (Blow 1993, 2001; Coverley et al. 1993). However, to date there is no evidence to support a relationship with this group of proteins.

In this paper, we report a correlation between 60-kDa LFM-1 polypeptide and cancer phenotype. Cancer cells in contrast with non-tumorigenic or normal tissues exhibited only one single (mostly unique) 60-kDa LFM-1 band defectively associated with chromosomes. Consistently, LFM-1 subcellular distribution in nuclear peripheral areas of potential telomere segregation, and decreased chromosome labeling observed in cancer cells, suggest a potential dysfunction in cell-cycle-related events. It is suggestive of the telomeric localization of LFM-1 protein and the data in the literature reporting regulatory functions of telomeres and telomerase activity on cell proliferation (Price 1992; Harley 1992; Jacob et al. 2001). In this regard, other chromosomal-scaffolding components such as RAP-1, a 116-kDa abundant protein with a role in the control of DNA proliferation (Klein et al. 1992), also termed TUF (Vignais and Sentenac 1989), and GRF-1 (Shuey and Parker 1986), have been reported to be mainly bound to telomeric areas. Also, CAP, a chromosomal auxiliary protein with similar chromosome binding to LFM-1, has been reported to play a role in DNA-bending at specific sites during gene regulation in yeast (Liu-Johnson et al. 1986), activating genes essential for the initiation of DNA replication (Koepsel and Khan 1986), and preventing telomere-telomere joining and degradation (Bourgain and Katinka 1991).

During the last few years, changes in the nuclear matrix have been reported in cancer cells. Malignancy-related two-dimensional gel spots have been described in a variety of human cancers (Keesee et al. 1994; Getzember and Coffey 1991; Kanuja et al. 1993). Despite these findings not yet having been assessed for specific cancer-related function(s), the study of these polypeptides may open a new avenue in the understanding of cancer biology and its potential treatment as well. The consistent results reported in this work on LFM-1 in a broad range of human malignancies suggest that 60-kDa LFM-1 polypeptide can be involved in malignant cell proliferation events. It is still hard to ascertain whether LFM-1 differences detected in tumor cells play a role in the malignant phenotype or are just a consequence of defective metabolic pathways or regulatory processes in tumor cells. However, the correlation between LFM-1 60-kDa polypeptide and cancer phenotype leads to the possibility of a dysfunction of chromosome-matrix components in the deregulated cancer proliferation. Although the 58-kDa/60-kDa polypeptides could be more relevant to tumor biology (in the case of a potential relationship with similar oncogenes and tumor suppressor genes expressed in tumors), the reported changes in the LFM-1 post-translational polypeptide in cancer cells may shed new insights by suggesting unsuspected structural/regulatory function(s) in the cancer phenotype.

Acknowledgements The authors are grateful to Dr. Irwin Berman for his helpful comments; Drs. Azorides Morales, Scott Y. Sittler, Phillip Ruiz, and Mehrdad Nadji (Department of Pathology, University of Miami School of Medicine) for providing support for the analysis of human biopsies; and Mr. Rosendo Morera (Tissue Procurement Facility, Sylvester Comprehensive Cancer Center) and Mrs. Juana Alonso (Department of Dermatology, University of Miami, School of Medicine) for technical assistance. This work was supported by the Skin Cancer Collaborative Project with the Department of Dermatology (U.M.) and the Cancer and Tumor Program, HIV Program (Sylvester Comprehensive Cancer Center, U.M.) to D.V.-S. The experiments performed in this work comply with the current laws in the United States.

References

Berezney R, Coffey DS (1974) Identification of a nuclear protein matrix. Biochem Biophys Res Commun 60:1410–1417

Blow JJ (1993) Preventing re-replication of DNA in a single cell cycle: evidence for a replication licensing factor. J Cell Biol 122:993–1002

Blow JJ (2001) Control of chromosomal DNA replication in the early *Xenopus* embryo (Review). EMBO J 20:3293–3297

Bourgain FM, Katinka MD (1991) Telomeres inhibit end to end fusion and enhance maintenance of linear DNA molecules injected into the *Paramecium primaurelia* macro nucleus. Nucleic Acids Res 19:1541–1547

Brazas RM, Stillman DJ (1993) Identification and purification of a protein that binds DNA cooperatively with the yeast SWI5 protein. Mol Cell Biol 13:5524–5537

Coverley D, Downes S, Romanowsky P, Laskey RA (1993) Reversible effects of nuclear membrane permeabilization on DNA replication: evidence for a positive licensing factor. J Cell Biol 122:985–992

de Belle I, Cai S, Kohwi-Shigematsu T (1998) Genomic sequences bound to special AT-rich sequence-binding protein 1 (SATB1) in vivo in Jurkat T cells are tightly associated with the nuclear matrix at the bases of the chromatin loops. J Cell Biol 141: 335–348

Dickinson LA, Dickinson CD, Kohwi-Shigematsu T (1992) A tissue-specific MAR/SAR DNA binding protein SATB1 contains a homeo-domain that promotes specific recognition of the core unwinding element of a MAR. Cell 70:631–645

Dijkwel PA, Wenink PW, Poddighe P (1986) Permanent attachment of replication origins to the nuclear matrix in BHK cells. Nucleic Acids Res 14:3241–3249

Dijkwel PA, Vaughn JP, Hamlin JL (1991) Mapping of replication initiation sites in mammalian genomes by two-dimensional gel analysis: stabilization and enrichment of replication intermediates by isolation on the nuclear-matrix. Mol Cell Biol 11: 3850–3859

Dohrman PR, Butler G, Tamai K, Dorland D, Greene JR, Thiele DJ, Stillman DJ (1992) Parallel pathways of gene regulation: homologous regulators SWI5 and ACE2 differentially control transcription of the HO and chitinase. Genes Dev 6:93–104

Durkin JP, Whitfield JF (1984) Partial characterization of the mitogenic action of $pp60^{v\text{-}src}$, the oncogenic protein product of the src gene of avian virus. J Cell Physiol 120:135–145

Earnshaw WC, Halligan B, Cooke CA, Heck MMS, Liu LF (1985) Topoisomerase II is a structural component of mitotic chromosome scaffolds. J Cell Biol 100:1706–1715

Elvira M, Diez JA, Wang KK, Villalobo A (1993) Phosphorylation of connexin-32 by protein kinase C prevents its proteolysis by mu-calpain and m-calpain. Biol Chem 268:14294–14300

Gasser SM, Laemmli UK (1987) Improved methods for the isolation of individual clustered mitotic chromosomes. Exp Cell Res 173:85–98

Gasser SM, Laroche T, Falquet J, Boy de la Tour E, Laemmli UK (1986) Metaphase chromosome structure. Involvement of topoisomerase II. J Mol Biol 188:613–629

Gasser SM, Amati BB, Cardenas ME, Hofman JF-X (1989) Studies on scaffold attachment sites and their relation to genome function. Int Rev Cytol 119:57–96

Getzember RH, Coffey DS (1991) Identification of nuclear matrix proteins in the cancerous and normal rat prostate. Cancer Res 51:6514–6520

Getzember RH, Konety BR, Oeler TA, Quiley MM, Hakam A, Becich MJ, Bahanson RR (1996) Bladder cancer-associated nuclear matrix proteins. Cancer Res 56:1690–1694

Guadagno JP, Assoian RK (1991) G_1/S control of anchorage-dependent growth in the fibroblast cell cycle. J Cell Biol 115: 1419–1425

Hamlin JL (1992) Mammalian origin of replication. Bioessays 14: 651–659

Harley CB (1992) Telomere loss: mitotic clock or genetic time bomb? Mutat Res 256:271–282

Hatakeyama M, Weinberg RA (1995) The role of Rb in cell control. Prog Cell Cycle Res 1:9–19

Hennesy KM, Clark CD, Botstein D (1990) Sub-cellular localization of yeast CDC46 varies with the cell cycle. Genes Dev 4: 2252–2263

Hernandez-Verdun D, Gautier T (1994) The chromosome periphery during mitosis. Bioessays 16:179–185

Hirano T, Mitchison MJ (1991) Cell-cycle control of higher-order chromatin assembly around naked DNA in vitro. J Cell Biol 115:1479–1489

Jacob NK, Skopp R, Price CM (2001) G-overhanging dynamics at *Tetrahymena* telomeres. EMBO J 20:4299–4308

Johnson DV, Foley NG (1993) Calpain-mediated proteolysis of microtubule-associated protein 2 (MAP-2) is inhibited by phosphorylation by camp-dependent protein kinase, but not by Ca^{2+}/calmodulin-dependent protein kinase II. J Neurosci Res 34:642–647

Kanuja PS, Lehr LE, Soule HD, Gehani SK, Noto AC, Choudhury S, Chen R, Pienta JK (1993) Nuclear matrix proteins in normal and breast cancer cells. Cancer Res 53:3394–3398

Keesee SK, Meneghini M, Szaro RP, Wu Y-J (1994) Nuclear matrix proteins in colon cancer. Proc Natl Acad Sci USA 91: 1913–1916

Kirchner MW (1992) The biochemical nature of the cell cycle (review). Important Adv Oncol 3–16

Klein F, Laroche T, Cardenas ME, Hofman JF-X, Schweizer D, Gasser SM (1992) Localization of Rap-1 and topoisomerase II in nuclei and meiotic chromosomes of yeast. J Cell Biol 117: 935–948

Koepsel RR, Khan SA (1986) Static and initiator protein-enhanced bending of DNA at replication origin. Science 233:1316–1318

Laemmli UK (1970) Cleavage of structural proteins during the assembly of bacteriophage T4. Nature 227:680–685

Liu-Johnson H-N, Gartenberg MR, Crothers DM (1986) DNA binding domain and bending angle of *E. coli* CAP protein. Cell 47:995–1005

Luscher B, Eisenman RN (1992) Mitosis-specific phosphorylation of the nuclear oncoproteins Myc and Myb. J Cell Biol 118:775–784

Madine MA, Khoo C-Y, Mills AD, Laskey RA (1995) MCM3 complex required for cell regulation of DNA replication in vertebrate cells. Nature 375:421–424

Mirkovich J, Mirau ME, Laemmli UK (1984) Organization of the higher-order chromatin loop: specific DNA attachment sites on nuclear scaffold. Cell 39:223–232

Nasmyth KG, Adolf G, Lydall D, Seddon A (1991) The identification of a second cell cycle control on the HO promoter in yeast: cell cycle regulation of SWI5 nuclear entry. Cell 62:631–647

Ng Y-K, Taborn G, Ahmad I, Radosevitch J, Bauer K, Iannaccone P (1992) Spatio-temporal changes in Ha-ras p21 expression through the hepatocyte cell-cycle during liver regeneration. Dev Biol 150:352–362

Nishimoto T, Ishida R, Ajiro K, Yamamoto S, Takahashi T (1981) The synthesis of protein(s) for chromosome condensation may be regulated by a post-transcriptional mechanism. J Cell Physiol 109:299–308

Paulson JR, Laemmli UK (1977) The structure of histone-depleted metaphase chromosomes. Cell 12:817–828

Pernov A, Bavykin S, Hamlin JL (1998) Attachment to the nuclear matrix mediates specific alterations in chromatin structure. Proc Natl Acad Sci U S A 95:14757–14762

Prevostel C, Alvaro V, Vallentin A, Martin A, Jaken S, Joubert D (1998) Selective loss of substrate recognition induced by the tumor-associated D294G point mutation in protein kinase C alpha. Biochem J 334:393–397

Price CM (1992) Centromeres and telomeres. Curr Opin Cell Biol 4:379–384

Reddy BA, Kloc M, Etkin L (1991) The cloning and characterization of a maternally expressed novel zinc finger nuclear phosphoprotein (xnf7) in *Xenopus laevis*. Dev Biol 148:107–116

Saitoh N, Goldberg IG, Earnshaw WC (1995) The SMC proteins and the coming of the age of the chromosome scaffold hypothesis. Bioessays 17:759–766

Saville MK, Watson RJ (1998) The cell-cycle regulated transcription factor B-Myb is phosphorylated by cyclin A/Cdk2 at sites that enhance its trans-activation properties. Oncogene 17:2679–2689

Shuey DJ, Parker CS (1986) Bending of promoter DNA on binding of heat shock transcriptor factor. Nature 323:459–461

Soule HD, Vasquez J, Long A, Albert S, Brennan M (1973) A human cell line from a pleural effusion derived from a breast carcinoma. J Natl Cancer Inst 51:1409–1413

Soule HD, Maloney TM, Wolman SR, Peterson WD, Brenz R, McGrath CM, Russo J, Pauley RJ, Jones RF, Brooks SC (1990) Isolation and characterization of a spontaneously immortalized human breast epithelial cell line, MCF-10. Cancer Res 50:6075–6086

Stein GS, Stein JL, Lian JB, van Wijnen AJ, Montecino M (1996) Functional interrelationships between nuclear structure and transcriptional control: contributions to regulation of cell-cycle, and tissue-specific gene expression. J Cell Biochem 62: 198–209

Stillman DJ, Bankier AT, Seddon A, Groenhout EG, Nasmyth KA (1988) A characterization of a transcription factor involved in mother cell specific transcription of the yeast HO gene. EMBO J 7:485–494

Subramanian D, Rosenstein BS, Muller M (1998) Ultraviolet-induced DNA damage stimulates topoisomerase I-DNA complex formation in vivo: possible relationship with DNA repair. Cancer Res 58:976–984

Swarup G, Radha V (1992) Protein tyrosine phosphatases as regulators of protein kinase activity. Curr Sci 62:462–469

Takeichi M (1993) Cadherins in cancer: implications for invasion and metastasis. Curr Opin Cell Biol 5:806–811

Towbin H, Staehelin T, Gordon J (1979) Electrophoretic transfer of proteins from polyacrylamide gels to nitrocellulose sheets: procedure and some applications. Proc Natl Acad Sci USA 76:4350–4354

Tyers M, Tokiwa G, Nash R, Futcher B (1992) The ClnCdc28 kinase complex of *S. cerevisiae* is regulated by proteolysis and phosphorylation. EMBO J 11:1773–1784

Uemura T, Ohkura H, Adachi Y, Morino K, Shiozaki K, Yanagida M (1987) DNA topoisomerase II is required for condensation and separation of mitotic chromosomes in *S. pombe*. Cell 50: 917–925

Vega-Salas DE, Salas PJI (1996) Cell cycle related behavior of a chromosomal-scaffold protein in MDCK epithelial cells. Chromosoma 104:321–331

Vega-Salas DE, Salas PJI, Gundersen D, Rodriguez-Boulan E (1987) Formation of the apical pole of epithelial (Madin Darby canine kidney) cells: polarity of an apical protein is independent of tight junctions while segregation of a basolateral marker requires cell-cell interactions. J Cell Biol 104:905–916

Vignais ML, Sentenac A (1989) Asymmetric DNA bending induced by the yeast multi-functional factor TUF. J Biol Chem 264:8463–8466

Von Kries JP, Buhrmeister H, Stratling WH (1991) A matrix/scaffold attachment region binding protein: identification, purification and mode of binding. Cell 64:123–135

Wei X, Samarabandu J, Devdhar RS, Siegel AJ, Acharya R, Berezney R (1998) Segregation of transcription and replication sites into higher order domains. Science 281:1502–1506

Wright SJ, Shatten G (1990) Teniposide, a topoisomerase II inhibitor, prevents chromosome condensation and separation but not decondensation in fertilized surf clam (*Spisula solidissima*) oocytes. Dev Biol 142:224–232

Yanagisawa J, Ando J, Nakayama J, Kohwi Y, Kohwi-Shigematsu T (1996) A matrix attachment region (MAR)-binding activity due to a p114 kilodalton protein is found only in human breast carcinomas and not in normal and benign breast disease tissues. Cancer Res 56:457–462

Yang L, Yam HF, Cheng-Chew SB, Wong SW, Loong EPL, Chew EC (1997) The association of HPV16 DNA with specific nuclear matrix proteins of normal and cervical carcinoma cells. Anticancer Res 17:343–348

Zeng C, van Wijnen AJ, Stein JL, Meyers S, Sun W, Shopland L, Lawrence JB, Penman S, Lian JB, Stein GS, Hiebert SW (1997) Identification of a nuclear matrix targeting signal in the leukemia and bone-related AML/CBF-a transcription factors. Proc Natl Acad Sci U S A 94:6746–6751

Zlatanova JS, van Holde KE (1992) Chromatin loops and transcriptional regulation. Crit Rev Eukaryot Gene Expr 2: 211–224